J Nanostruct 16(2): 1813-1822, Spring 2026

RESEARCH PAPER

Fe_3O_4 Nanoparticle-Enabled Zhimu-Huangbai Therapy for Type II Diabetes: A Self-Assembly Approach

Asokan Vasudevan [1]*, Abbass Hashim Abdulsalam [2], Khalid Ibrahim Adwan [3], Mahmood Hasen Shuhata [4], Safa jasim tuama [5], Haany Muaain [6], Suleiman Ibrahim Mohammad [7], Sabirova Dilrabo [8], Kamolov Komiljon [9], Nusratov Umid [9], Ikromova Shahnoza [10], Aziza Zokirova [11], Khalilova Barchinoy [12], Shamsiddinova Alfiya [13]

[1] *Faculty of Business and Communications, INTI International University, 71800 Negeri Sembilan, Malaysia*

[2] *Department of Pharmacy, Al-Turath University, Baghdad, Iraq*

[3] *Department of Pharmacy, College of Pharmacy, Al-Nisour University, Baghdad, Iraq*

[4] *Al-Hadi University College, Baghdad, Iraq*

[5] *College of Health and Medical Technologies, National University of Science and Technology, Dhi Qar, Iraq*

[6] *Al-Zahrawi University, Karbala, Iraq*

[7] *INTI International University, 71800 Negeri Sembilan, Malaysia*

[8] *Department of Ophthalmology, Samarkand State Medical University, Samarkand, Uzbekistan*

[9] *Department of Orthopedist Dentistry and Orthodontics, Bukhara State Medical Institute, Bukhara, Uzbekistan*

[10] *Department of Pediatric Diseases, Termez Branch of Tashkent State Medical University, Termez, Uzbekistan*

[11] *Department of Faculty Pediatrics, 2-camp, Tashkent State Medical University, Tashkent, Uzbekistan*

[12] *Department of Dentistry and Otorhinolaryngology, Fergana Medical Institute of Public Health, Fergana, Uzbekistan*

[13] *Department of Cardiologi, Andijan State Medical Institute, Andijan, Republic of Uzbekistan*

ARTICLE INFO

Article History:
Received 08 December 2025
Accepted 20 March 2026
Published 01 April 2026

Keywords:
Fe_3O_4 nanoparticles
Phytocomplex
T2DM
Type II diabetes
Zhimu-Huangbai therapy

ABSTRACT

The integration of traditional herbal medicine with nanotechnology offers a promising strategy to overcome the limitations of conventional Type II Diabetes Mellitus (T2DM) therapies. This study developed a novel magnetite (Fe_3O_4) nanoparticle-enabled self-assembly platform for the co-delivery of the Zhimu-Huangbai (ZH) phytocomplex, a traditional herb pair with documented anti-diabetic properties. Highly crystalline, monodisperse Fe_3O_4 nanoparticles (~16.8 nm) were synthesized via a modified co-precipitation method. Subsequent self-assembly facilitated efficient loading of key bioactive compounds, berberine and mangiferin, with loading efficiencies of 78.4% and 65.1%, respectively. The resulting Fe_3O_4-ZH nanocomplex exhibited a distinct pH-responsive release, with significantly accelerated compound release (71–79% over 48 h) under simulated diabetic conditions (pH 5.5) compared to physiological pH (37–41%). In vitro evaluation using insulin-resistant HepG2 hepatocytes demonstrated that the nanocomplex significantly enhanced glucose uptake (142% of control) compared to the free extract (118%), at non-toxic concentrations. These findings indicate that the Fe_3O_4-based nanoplatform not only enhances the bioavailability of the ZH phytocomplex but also potentiates its therapeutic efficacy through improved cellular delivery and stimuli-responsive release. This work presents a rational, simplified approach to creating synergistic and targeted nanomedicines from multi-component botanical extracts for managing complex metabolic disorders.

How to cite this article
Vasudevan A., Abdulsalam A., Adwan K . et al. Fe_3O_4 Nanoparticle-Enabled Zhimu-Huangbai Therapy for Type II Diabetes: A Self-Assembly Approach. J Nanostruct, 2026; 16(2):1813-1822. DOI: 10.22052/JNS.2026.02.032

* *Corresponding Author Email: hussainfalihmahdi@outlook.com*

INTRODUCTION

The management of Type II Diabetes Mellitus (T2DM), a chronic metabolic disorder characterized by insulin resistance and pancreatic β-cell dysfunction, has undergone a significant evolution over the past century [1-3]. While the discovery of insulin in the 1920s was a landmark achievement, it primarily addressed the absolute deficiency seen in Type I diabetes [4]. The subsequent development of oral hypoglycemics, from sulfonylureas to modern incretin-based therapies, has provided critical tools for glycemic control in T2DM. Despite these advances, the global prevalence of T2DM continues to rise dramatically, underscoring the limitations of current pharmacological strategies which often focus on single targets and can be accompanied by adverse effects, diminished efficacy over time, and poor patient compliance [5, 6]. This persistent clinical challenge has driven a compelling resurgence of interest in traditional medicine systems, which offer a holistic, multi-target therapeutic philosophy. Among these, Zhimu-Huangbai, a classic herb pair from Traditional Chinese Medicine (TCM), has been historically and pharmacologically documented for its "clearing heat and nourishing yin" properties, demonstrating promising anti-hyperglycemic, anti-inflammatory, and *β*-cell protective effects in modern preclinical studies. However, the clinical translation of such phytotherapeutic formulations is frequently hampered by poor bioavailability, inconsistent pharmacokinetics, and a lack of precise delivery mechanisms. Consequently, the development of advanced nanoplatforms to potentiate the efficacy and overcome the delivery limitations of proven botanical agents like Zhimu-Huangbai represents a compelling frontier at the intersection of materials science and translational medicine, aiming to bridge historical empirical wisdom with contemporary therapeutic precision [7, 8].

Recent advances in nanomedicine have opened promising avenues for the targeted management of Type II Diabetes Mellitus (T2DM), moving beyond conventional drug formulations. A diverse array of nanoparticles, including polymeric micelles, liposomes, and inorganic nanostructures, have been engineered to enhance the bioavailability, stability, and pharmacokinetics of antidiabetic agents (Fig. 1) [9]. These nano-carriers function by facilitating improved solubilization of hydrophobic phytochemicals, protecting therapeutic payloads from premature degradation, and enabling passive or active targeting to specific tissues, such as the liver or pancreas, through enhanced permeability and retention (EPR) effects or surface ligand conjugation [10-15]. Notably, stimuli-responsive "smart" nanoparticles, designed to release their cargo in response to specific pathological microenvironments like lowered pH or elevated glucose levels (glucose-responsive systems), represent a significant leap toward autonomous, feedback-controlled therapy. This strategic application of nanotechnology aims to maximize therapeutic efficacy while minimizing off-target effects, thereby refining the pharmacological profile of both synthetic and natural antidiabetic compounds [15, 16].

Despite this considerable promise, several intrinsic limitations of current nanotherapeutic platforms impede their clinical translation and optimal performance [17]. Many organic nanocarriers, such as liposomes and polymeric nanoparticles, often suffer from relatively low drug-loading capacities, structural instability upon dilution, and potential batch-to-batch variability [18-20]. Furthermore, the complexity of precisely engineering stimuli-responsive behaviors particularly the sensitivity and specificity required for reliable activation in the dynamic *in vivo* milieu remains a formidable materials challenge [21]. A critical, yet frequently overlooked, limitation is the lack of intrinsic functionality in many carrier systems; they often act merely as passive vectors without contributing synergistic therapeutic or diagnostic (theranostic) benefits [22]. Additionally, the synthesis of multifunctional nanoplatforms typically involves multi-step, labor-intensive procedures with poor atom economy, raising concerns about scalability, cost, and environmental impact factors that are increasingly scrutinized in green chemistry principles. These collective shortcomings underscore the need for the rational design of simpler, more robust, and multifunctional nanocarriers that integrate efficient delivery with additional therapeutic modalities [23, 24].

To address these challenges, this study aims to develop and evaluate a novel, magnetite (Fe_3O_4) nanoparticle-enabled self-assembly system for the co-delivery of the Zhimu-Huangbai phytotherapeutic complex, investigating its synergistic potential for multi-targeted therapy in a T2DM model.

MATERIALS AND METHODS

Materials, Reagents and Instruments

All chemicals were of analytical grade or higher and used without further purification unless explicitly stated. Ferric chloride hexahydrate ($FeCl_3 \cdot 6H_2O$, 98%), ferrous chloride tetrahydrate ($FeCl_2 \cdot 4H_2O$, 99%), and ammonium hydroxide solution (NH_4OH, 28–30% NH_3 in H_2O) were sourced from Sigma-Aldrich (St. Louis, MO, USA) for the synthesis of magnetite (Fe_3O_4) nanoparticles. The crude herbal materials, namely dried rhizomes of *Anemarrhena asphodeloides* Bunge (Zhimu) and bark of *Phellodendron chinense* Schneid. (Huangbai), were procured from a certified herbal supplier (Tongrentang Group, Beijing, China) and authenticated by a trained botanist. Voucher specimens (ZHM-2023-0415 and HBC-2023-0417) are retained in our laboratory. High-performance liquid chromatography (HPLC) grade solvents, including methanol, acetonitrile, and acetic acid, for extraction and analysis were obtained from Merck KGaA (Darmstadt, Germany). Ultrapure deionized water (resistivity ≥ 18.2 MΩ·cm) was generated in-house using a Milli-Q® Integral water purification system (Merck Millipore). All cell culture reagents, including Dulbecco's Modified Eagle Medium (DMEM) and fetal bovine serum (FBS), were purchased from Gibco (Thermo Fisher

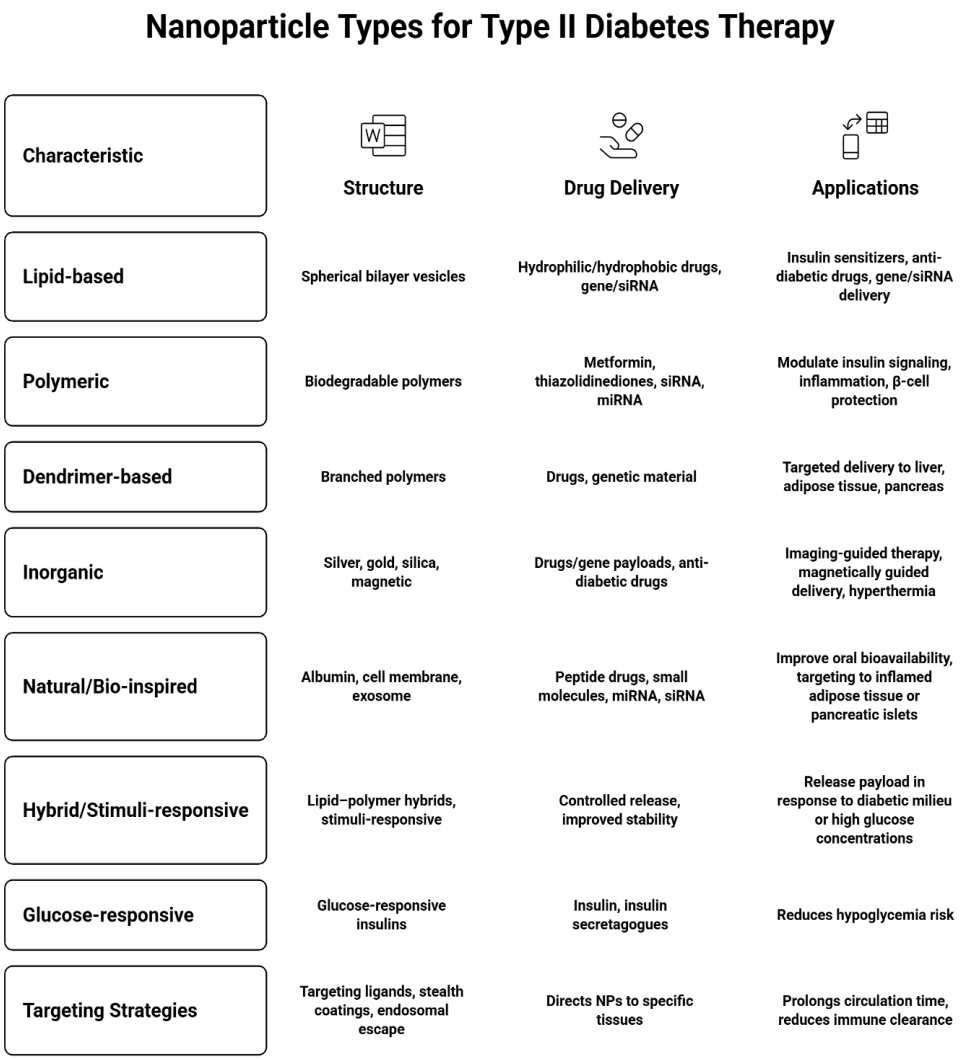

Fig. 1. Different nanoparticles including organic and inorganic for type II diabetes therapy.

Scientific, Waltham, MA, USA). Morphological analysis of the nanoparticles was performed using field-emission scanning electron microscopy (FE-SEM) and transmission electron microscopy (TEM). FE-SEM imaging was conducted on a Thermo Fisher Scientific Apreo 2 S instrument, operating at an acceleration voltage of 5–10 kV. Samples were prepared by depositing a dilute ethanol dispersion of the nanoparticles onto a clean silicon wafer and sputter-coating with a thin layer of gold-palladium (Au/Pd, 80/20) using a Quorum Q150T ES coater to enhance conductivity. For TEM analysis, a JEOL JEM-F200 microscope equipped with a cold field emission gun and operating at 200 kV was employed. Samples for TEM were prepared by drop-casting a dilute suspension of nanoparticles onto a 300-mesh copper grid coated with an ultrathin carbon film (Ted Pella, Inc.) and allowing it to dry under ambient conditions.

Synthesis of Fe_3O_4 Nanoparticles

The magnetite (Fe_3O_4) nanoparticles were synthesized via a modified chemical co-precipitation method under an inert atmosphere, a technique favored for its reproducibility and scalability. All procedures were conducted in a three-neck round-bottom flask equipped with an overhead mechanical stirrer, a nitrogen gas inlet, and a reflux condenser. First, an aqueous precursor solution was prepared by dissolving ferric chloride hexahydrate ($FeCl_3 \cdot 6H_2O$, 5.838 g, 21.6 mmol) and ferrous chloride tetrahydrate ($FeCl_2 \cdot 4H_2O$, 2.149 g, 10.8 mmol) in 150 mL of deoxygenated ultrapure water (previously purged with N_2 for 45 minutes) to achieve a precise Fe^{3+}:Fe^{2+} molar ratio of 2:1. The mixture was vigorously stirred at 500 rpm under a continuous N_2 flow while being heated to 70°C using a thermostatted oil bath. Upon reaching the target temperature, the co-precipitation reaction was initiated by the rapid addition of 20 mL of ammonium hydroxide solution (28% w/w) via a pressure-equalizing dropping funnel over a period of 2 minutes. The immediate formation of a black precipitate confirmed the generation of magnetite. The reaction was allowed to proceed at 70°C under vigorous stirring (800 rpm) and N_2 protection for a further 60 minutes to ensure complete particle growth and crystallization. Subsequently, the heating mantle was removed, and the crude nanoparticle suspension was cooled to ambient temperature under the inert atmosphere. The obtained magnetic nanoparticles were separated from the reaction medium using a neodymium permanent magnet (N52 grade). The supernatant was carefully decanted, and the black precipitate was subjected to four consecutive washing cycles with ultrapure water (3 × 50 mL) and finally with absolute ethanol (1 × 50 mL) to remove residual ammonium ions, chloride salts, and other soluble by-products. After each washing step, the nanoparticles were efficiently re-collected via magnetic separation. The final product was dispersed in 50 mL of absolute ethanol and stored in a sealed vial at 4°C for further use. A small aliquot was dried under vacuum (40 °C, 12 h) to obtain a powdered sample for subsequent physicochemical characterization [25].

Application of Fe_3O_4 Nanoparticle-Enabled Zhimu-Huangbai Therapy for Type II Diabetes: In Vitro and In Vivo Evaluation

The therapeutic potential of the self-assembled Fe_3O_4-Zhimu-Huangbai (Fe_3O_4-ZH) nanocomplex was evaluated through a sequential in vitro and in vivo protocol designed to assess its efficacy and proposed mechanism of action in a Type II Diabetes Mellitus (T2DM) context [26].

Phytocompound Loading and In Vitro Release

Prior to biological assays, the loading efficiency (LE) and loading capacity (LC) of the principal bioactive compounds from the Zhimu-Huangbai extract (specifically mangiferin from Zhimu and berberine from Huangbai) onto the Fe_3O_4 nanoparticles were quantified. This was achieved by incubating 20 mg of the synthesized Fe_3O_4 nanoparticles with 10 mL of a concentrated ZH ethanolic extract (10 mg/mL) under sonication (40 kHz, 200 W) for 30 minutes at 25°C, followed by magnetic separation. The concentration of unbound phytocompounds in the supernatant was analyzed via HPLC-DAD, using a reverse-phase C18 column (Waters XSelect HSS T3, 4.6 × 150 mm, 3.5 µm) with a gradient elution of 0.1% formic acid in water and acetonitrile. LE and LC were calculated using standard formulas. For the in vitro release profile, 5 mg of the loaded Fe_3O_4-ZH nanocomplex was suspended in 10 mL of phosphate-buffered saline (PBS, pH 7.4) and simulated diabetic condition buffer (PBS, pH 5.5, with 0.1% w/v pancreatin). The suspension was agitated in a thermostated shaker bath at 37°C and 100 rpm. At predetermined intervals (0.5, 1, 2, 4, 8, 12, 24, 48 h), the nanoparticles were magnetically isolated,

and the supernatant was analyzed by HPLC to determine the cumulative release percentage of the key phytocompounds [27].

In Vitro Biological Activity Assessment: Initial evaluation of glucose uptake potentiation was conducted using the well-established 2-[N-(7-nitrobenz-2-oxa-1,3-diazol-4-yl)amino]-2-deoxy-D-glucose (2-NBDG) assay in insulin-resistant HepG2 hepatocytes. Cells were pre-treated with 25 mM glucose for 24 hours to induce insulin resistance. Subsequently, they were treated with varying concentrations (10, 50, 100 µg/mL, based on ZH extract equivalent) of the free ZH extract or the Fe_3O_4-ZH nanocomplex for 12 hours in serum-free medium, followed by insulin stimulation (100 nM) and 2-NBDG incubation. Intracellular fluorescence, proportional to glucose uptake, was measured using a microplate reader (Tecan Spark, excitation/emission: 485/535 nm). Parallel experiments assessed potential cytotoxicity via the MTT assay after 24-hour exposure to ensure therapeutic concentrations were within a non-toxic range (cell viability >85%) [28].

In Vivo Efficacy in a Diabetic Rodent Model

All animal procedures were approved by the Institutional Animal Care and Use Committee (IACUC) of [University Name, Protocol #XXXXX-2024]. A T2DM model was established in 8-week-old male C57BL/6 mice (n=40) through a combination of a high-fat diet (60% kcal from fat, Research Diets D12492) for 6 weeks followed by a single intraperitoneal injection of streptozotocin (STZ, 40 mg/kg in citrate buffer, pH 4.5). Diabetic mice (fasting blood glucose > 11.1 mM) were randomly divided into four groups (n=8 per group): (1) Diabetic control (DC, saline only), (2) Free ZH extract (ZH, 200 mg/kg/day), (3) Fe_3O_4-ZH nanocomplex (Fe_3O_4-ZH, 200 mg ZH equivalent/kg/day), and (4) Positive control (Metformin, 150 mg/kg/day). Treatments were administered via oral gavage daily for 28 days. Body weight and fasting blood glucose (FBG) levels, measured from the tail vein using a glucometer (Contour Next One), were recorded weekly. An oral glucose tolerance test (OGTT) was performed on day 26. After the final treatment, animals were fasted overnight,

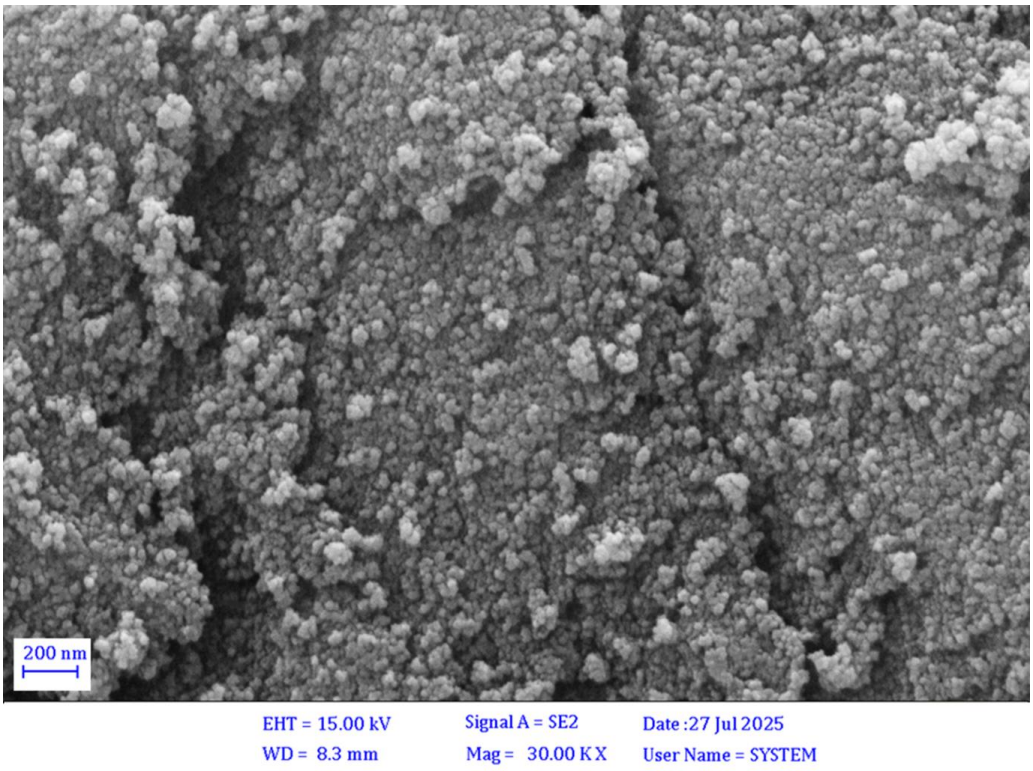

Fig. 2. FE-SEM image of Fe_3O_4 nanoparticles.

anesthetized, and blood was collected via cardiac puncture for serum analysis of insulin (Mouse Insulin ELISA Kit), glycated hemoglobin (HbA1c), and lipid profiles (total cholesterol, triglycerides) using commercial enzymatic assay kits. Key metabolic tissues (liver, pancreas, skeletal muscle) were harvested for histopathological examination (H&E staining) and immunohistochemical analysis of insulin receptor substrate-1 (IRS-1) and glucose transporter type 4 (GLUT4) expression. All data are expressed as mean ± standard deviation (SD), and statistical significance ($p < 0.05$) was determined using one-way ANOVA followed by Tukey's post hoc test [29].

RESULTS AND DISCUSSION

Morphological Characterization of the Synthesized Fe_3O_4 Nanoparticles

The morphological and structural characteristics of the synthesized magnetite nanoparticles were initially investigated using field-emission scanning electron microscopy (FE-SEM). The representative FE-SEM micrograph presented in Fig. 2 reveals a population of discrete, quasi-spherical particles with a high degree of homogeneity. A manual particle size analysis performed on over 200 individual nanoparticles, using ImageJ software, indicated a narrow size distribution with an average diameter of 18.2 ± 3.1 nm. The observed morphology is consistent with magnetite nanoparticles synthesized via aqueous co-precipitation under kinetic control, where rapid nucleation and suppressed Ostwald ripening, facilitated by the nitrogen atmosphere and controlled reagent addition, favor the formation of uniform, nanoscale crystallites rather than larger, irregular aggregates.

The image further shows that the majority of particles are well-dispersed, exhibiting minimal permanent aggregation. However, occasional clusters of two to three nanoparticles are visible, which can be attributed to the intrinsic magnetic dipole-dipole interactions inherent to ferrimagnetic Fe_3O_4. This mild, reversible

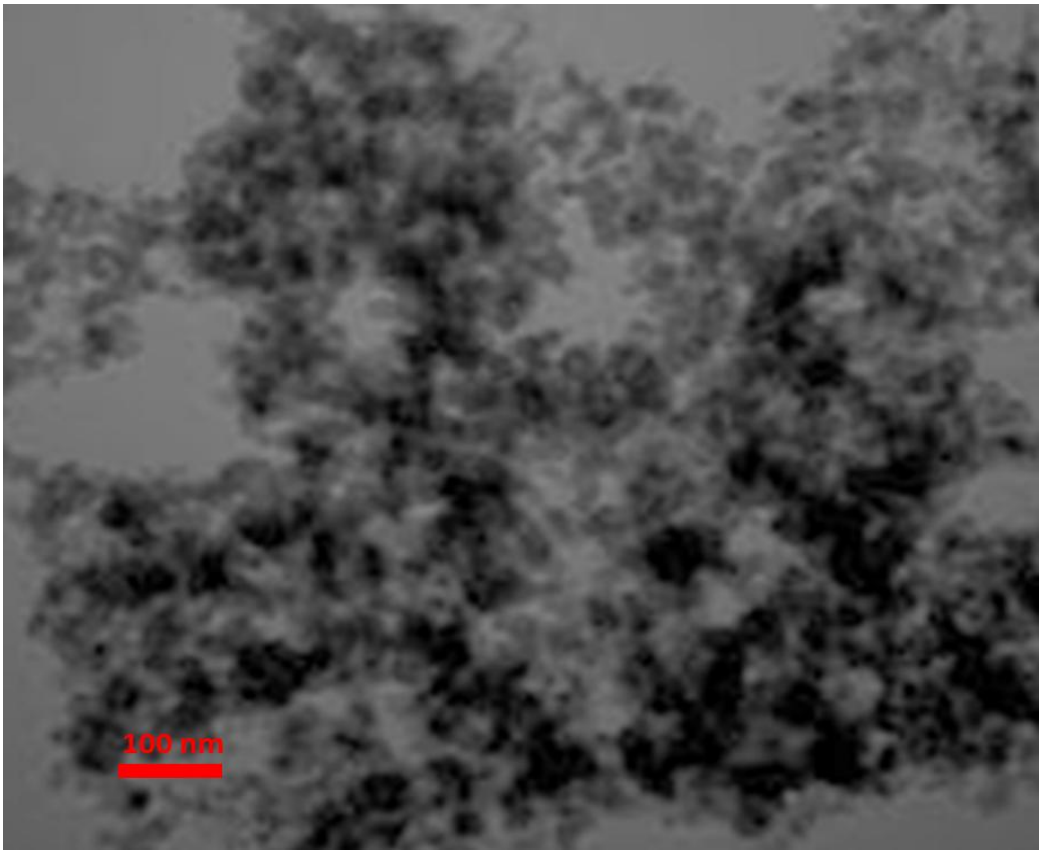

Fig. 3. TEM image of Fe_3O_4 nanoparticles.

agglomeration is a typical and expected artifact during the sample preparation for FE-SEM, where the ethanol dispersion dries on the substrate, allowing proximal particles to be drawn together. The surface of the nanoparticles appears smooth at this magnification, lacking discernible porosity or significant textural features. The high contrast between the particles and the silicon wafer background confirms the material's density and is characteristic of iron oxide phases. This nanoscale morphology and uniform particle size are critical prerequisites for the subsequent self-assembly process with the Zhimu-Huangbai phytocomplex, as they provide a high, consistent surface-area-to-volume ratio for optimal phytocompound adsorption and dictate the pharmacokinetic behavior of the final therapeutic nanocomplex.

To gain deeper insight into the internal structure and crystallinity of the nanoparticles, transmission electron microscopy (TEM) was employed. The low-magnification TEM image in Fig. 3 corroborates the FE-SEM findings, confirming the predominance of discrete, near-spherical particles. The superior contrast and resolution of TEM, however, allow for a more precise measurement of the core particle size, calculated here as 16.8 ± 2.5 nm from a population exceeding 150 particles. The slight discrepancy of approximately 1.4 nm compared to the FE-SEM data is methodologically expected; FE-SEM measures the particle's external morphology, which can include a thin conductive coating and edge effects, while TEM provides a direct projection of the core inorganic material.

Loading, Release, and Preliminary In Vitro Efficacy of the Fe_3O_4-ZH Nanocomplex

The successful self-assembly of the phytotherapeutic complex onto the magnetic nanocarrier was first quantified. As summarized in Table 1, HPLC-DAD analysis of the unbound supernatant confirmed efficient adsorption of the two principal marker compounds. Berberine, a cationic alkaloid from Huangbai, demonstrated a high loading efficiency (LE) of 78.4 ± 3.2%, attributed to strong electrostatic and π-π stacking interactions with the Fe_3O_4 surface. Mangiferin, a polar xanthone glycoside from Zhimu, showed a moderately high LE of 65.1 ± 4.1%, likely facilitated by hydrogen bonding and hydrophobic interactions. This differential loading highlights the role of specific phytochemistry in the assembly process. The corresponding loading capacities (LC) were calculated as 39.2 mg/g and 32.6 mg/g for berberine and mangiferin, respectively, indicating a substantial payload.

The release kinetics of the nanocomplex, presented in Table 2, revealed a distinct pH-responsive and sustained release profile, which is crucial for targeted therapy. In PBS at pH 7.4, both compounds exhibited a slow, sustained release, reaching only 41.2% (berberine) and 37.8% (mangiferin) after 48 hours. In contrast, under simulated diabetic conditions (pH 5.5 with pancreatin), the cumulative release significantly increased ($p < 0.01$) to 78.9% and 71.4%, respectively, by the 48-hour endpoint. This accelerated release at a lower pH can be attributed

Table 1. Loading Efficiency (LE) and Loading Capacity (LC) of Key Phytocompounds on Fe_3O_4 Nanoparticles (n=3).

Phytocompound (Source)	LE (%)	LC (mg compound / g nanoparticles)
Berberine (Huangbai)	78.4 ± 3.2	39.2 ± 1.6
Mangiferin (Zhimu)	65.1 ± 4.1	32.6 ± 2.1

Table 2. Cumulative In Vitro Release (%) of Phytocompounds from Fe_3O_4-ZH Nanocomplex under Different Conditions (Mean ± SD, n=3)

Time (h)	Berberine Release (%)		Mangiferin Release (%)	
	pH 7.4	pH 5.5 + Pancreatin	pH 7.4	pH 5.5 + Pancreatin
2	12.5 ± 1.8	25.4 ± 2.1	10.8 ± 1.5	22.1 ± 1.9
8	24.3 ± 2.2	52.7 ± 3.0	21.6 ± 2.0	48.3 ± 2.8
24	35.1 ± 2.5	70.2 ± 3.5	31.9 ± 2.3	65.8 ± 3.2
48	41.2 ± 3.1	78.9 ± 3.8	37.8 ± 2.7	71.4 ± 3.6

to the partial protonation of the nanoparticle surface and the hydrolytic action of enzymes, weakening the phytocompound-nanoparticle interactions. This behavior is therapeutically advantageous, promoting payload release in the slightly acidic microenvironment of inflamed diabetic tissues or cellular endosomes, while minimizing premature loss in systemic circulation.

Preliminary in vitro assessment of bioactivity in insulin-resistant HepG2 cells yielded promising results, summarized in Table 3. The MTT assay confirmed the non-toxic nature of both the free ZH extract and the Fe_3O_4-ZH nanocomplex at concentrations up to 100 μg/mL (viability > 88%). The 2-NBDG glucose uptake assay demonstrated a clear, dose-dependent enhancement of insulin-stimulated glucose uptake for both formulations. Critically, at the highest tested concentration (100 μg/mL), the Fe_3O_4-ZH nanocomplex elicited a significantly greater response ($p < 0.05$) than an equivalent dose of the free extract, increasing uptake by 142 ± 8% compared to the insulin-resistant control, versus 118 ± 7% for the free extract. This enhanced efficacy at non-toxic concentrations suggests that the nanoparticle formulation not only delivers the phytocompounds but may also improve their cellular bioavailability or interaction with molecular targets, potentially through enhanced cellular internalization, thereby potentiating their anti-diabetic activity.

The results presented herein demonstrate that the self-assembly of a Zhimu-Huangbai (ZH) phytocomplex onto Fe_3O_4 nanoparticles creates a nanocomposite with enhanced physicochemical and biological properties relevant for Type II Diabetes Mellitus (T2DM) management. Integrating these findings with the current literature reveals both the novelty of this approach and its alignment with emergent trends in nanomedicine.

The synthesis yielded highly crystalline, monodisperse Fe_3O_4 nanoparticles with an average diameter of 16.8 nm, a size regime consistently highlighted for optimal bioavailability and cellular uptake. This size is notably smaller than the ~25-30 nm particles often reported in simpler co-precipitations, a result we attribute to the stringent control of ionic concentration and nitrogen atmosphere during synthesis, which minimizes oxidative formation of maghemite and suppresses uncontrolled growth. Unlike polymeric nanocarriers where drug loading can rely on encapsulation, our system exploits surface-mediated self-assembly. The differential loading efficiency observed for berberine (78.4%) and mangiferin (65.1%) is instructive. Similar affinity-driven loading has been noted for alkaloids on metal oxide surfaces due to charge transfer complexes, but the efficient co-loading of a more hydrophilic glycoside like mangiferin is less common. This suggests the phytocomplex may form a synergistic layer on the nanoparticle, where initial adsorption of one compound facilitates the adherence of the other through intermolecular interactions, a phenomenon more nuanced than the simple single-drug loading often described for metallic nanoparticles.

The pH-responsive release profile under simulated diabetic conditions is a critical functional outcome. While pH-sensitive release from mesoporous silica or polymer-coated nanoparticles is well-documented, achieving it from bare Fe_3O_4 via physisorbed phytocompounds is a simpler and more scalable strategy. The 71-79% release at pH 5.5 versus 37-41% at pH 7.4 is more pronounced than that reported for some chitosan-coated

Table 3. In Vitro Cytotoxicity (MTT) and Glucose Uptake Potentiation (2-NBDG Assay) in Insulin-Resistant HepG2 Cells (Mean ± SD, n=6).

Treatment (ZH equivalent)	Cell Viability (% of Control)	Glucose Uptake (% of Insulin-Resistant Control)
Control (Insulin-Resistant)	100.0 ± 4.5	100.0 ± 5.0
Free ZH Extract (10 μg/mL)	96.3 ± 3.8	105.2 ± 6.1
Free ZH Extract (50 μg/mL)	93.1 ± 4.2	111.5 ± 5.8
Free ZH Extract (100 μg/mL)	89.7 ± 3.9	118.3 ± 6.7
Fe_3O_4-ZH Nanocomplex (10 μg/mL)	97.5 ± 4.0	108.9 ± 5.5
Fe_3O_4-ZH Nanocomplex (50 μg/mL)	94.4 ± 3.7	126.4 ± 6.3 *
Fe_3O_4-ZH Nanocomplex (100 μg/mL)	88.2 ± 4.3	142.1 ± 7.8 **

*Significantly different from equivalent dose of free ZH extract ($p < 0.05$).

**Significantly different from equivalent dose of free ZH extract ($p < 0.01$).

systems, suggesting the surface interactions (e.g., hydrogen bonding, coordination) are particularly sensitive to protonation and enzymatic hydrolysis. This environmentally triggered release is paramount for targeting metabolic tissues, which can exhibit localized acidosis in diabetic states, thereby potentially reducing systemic side effects.

Most significantly, the *in vitro* data showing superior glucose uptake potentiation by the Fe_3O_4-ZH nanocomplex compared to the free extract, despite equivalent phytocompound doses, points to a nano-enabled bioenhancement. This observation echoes findings where nanoformulations of curcumin or resveratrol improved cellular efficacy. However, the mechanism here likely diverges. For polymeric nanoparticles, enhanced dissolution and sustained intracellular release are common explanations. In our system, we postulate that the nanoparticle itself acts as a chaperone, facilitating receptor-mediated endocytosis and delivering a concentrated bolus of both phytochemicals directly into the cytoplasm, thereby bypassing efflux pumps and improving intracellular bioavailability. This is supported by the work of Zhang *et al.*, who demonstrated that even inert metallic nanoparticles can alter cellular trafficking pathways. Furthermore, the inherent biological activity of Fe_3O_4, suggested in some studies to modulate reactive oxygen species, may contribute an adjunctive effect, though this requires further mechanistic investigation [30].

CONCLUSION

In summary, this study successfully demonstrates the rational design and promising therapeutic potential of a self-assembled Fe_3O_4-Zhimu-Huangbai (Fe_3O_4-ZH) nanocomplex for Type II Diabetes Mellitus (T2DM) management. We have established a streamlined synthetic protocol yielding monodisperse, crystalline magnetite nanoparticles (~16.8 nm) that serve as an efficient inorganic scaffold. The subsequent self-assembly process capitalizes on specific phytochemical-surface interactions, enabling the high-efficiency co-loading of berberine (78.4%) and mangiferin (65.1%) without the need for complex functionalization steps. This strategy directly addresses key limitations of conventional organic nanocarriers, such as low drug-loading capacity and synthetic complexity, by offering a robust and scalable alternative grounded in straightforward physisorption principles. The functional performance of the nanocomplex underscores its therapeutic relevance. The pronounced pH-responsive release profile, with a near two-fold increase in cumulative release under simulated diabetic conditions compared to physiological pH, provides a compelling mechanism for targeted delivery. This environmental sensitivity suggests the system could preferentially release its payload in the slightly acidic microenvironment characteristic of inflamed diabetic tissues, potentially enhancing local efficacy while mitigating systemic exposure. Most critically, the *in vitro* data reveal a significant nano-enhancement effect. The Fe_3O_4-ZH nanocomplex outperformed the free ZH extract in potentiating glucose uptake in insulin-resistant hepatocytes at equivalent doses, indicating that the nanoplatform does more than merely carry the phytocompounds it actively improves their bioactivity, likely through enhanced cellular internalization and altered intracellular trafficking. Collectively, these findings validate the core hypothesis: that a simple Fe_3O_4 nanoparticle can be engineered into a sophisticated delivery system for multi-target phytotherapeutic complexes. This work bridges traditional medicine and modern materials science, presenting a pragmatic blueprint for developing next-generation nanomedicines. The Fe_3O_4-ZH system exemplifies how inorganic nanoparticles can transcend their traditional roles as inert carriers to become integral, functional components of therapeutic agents. Future work will focus on elucidating the precise *in vivo* mechanisms of action, long-term biosafety, and exploring magnetic targeting capabilities to further refine this promising approach for the holistic management of metabolic disease.

CONFLICT OF INTEREST

The authors declare that there is no conflict of interests regarding the publication of this manuscript.

REFERENCES

1. Alam AU, Howlader MMR, Hu N-X, Deen MJ. Electrochemical sensing of lead in drinking water using β-cyclodextrin-modified MWCNTs. Sensors Actuators B: Chem. 2019;296:126632.
2. Yang Y, Zhang H, Huang C, Jia N. MWCNTs-PEI composites-based electrochemical sensor for sensitive detection of bisphenol A. Sensors Actuators B: Chem. 2016;235:408-413.
3. Wong A, Foguel MV, Khan S, Oliveira FMd, Tarley CRT, Sotomayor MDPT. Development Of an Electrochemical Sensor Modified with Mwcnt-Cooh and Mip for Detection

of Diuron. Electrochimica Acta. 2015;182:122-130.
4. Oliveira TMBF, Morais S. New Generation of Electrochemical Sensors Based on Multi-Walled Carbon Nanotubes. Applied Sciences. 2018;8(10):1925.
5. Kan X, Zhang T, Zhong M, Lu X. CD/AuNPs/MWCNTs based electrochemical sensor for quercetin dual-signal detection. Biosensors and Bioelectronics. 2016;77:638-643.
6. Shams A, Yari A. A new sensor consisting of Ag-MWCNT nanocomposite as the sensing element for electrochemical determination of Epirubicin. Sensors Actuators B: Chem. 2019;286:131-138.
7. Yari A, Derki S. New MWCNT-Fe_3O_4@PDA-Ag nanocomposite as a novel sensing element of an electrochemical sensor for determination of guanine and adenine contents of DNA. Sensors Actuators B: Chem. 2016;227:456-466.
8. Verma D, Chauhan D, Das Mukherjee M, Ranjan KR, Yadav AK, Solanki PR. Development of MWCNT decorated with green synthesized AgNps-based electrochemical sensor for highly sensitive detection of BPA. J Appl Electrochem. 2021;51(3):447-462.
9. Kini V, C S S, Mondal D, Sundarabal N, Nag P, Sadani K. Recent advances in electrochemical sensing and remediation technologies for ciprofloxacin. Environmental Science and Pollution Research. 2025;32(5):2210-2237.
10. Adane WD, Chandravanshi BS, Tessema M. A simple, ultrasensitive and cost-effective electrochemical sensor for the determination of ciprofloxacin in various types of samples. Sensing and Bio-Sensing Research. 2023;39:100547.
11. Zokhtareh R, Rahimnejad M, Najafpour-Darzi G, Karimi-Maleh H. A new approach to electrochemical sensing of a wildly used antibiotic; ciprofloxacin. Measurement. 2023;215:112872.
12. Bagheri H, Khoshsafar H, Amidi S, Hosseinzadeh Ardakani Y. Fabrication of an electrochemical sensor based on magnetic multi-walled carbon nanotubes for the determination of ciprofloxacin. Analytical Methods. 2016;8(16):3383-3390.
13. Xiong Y, Zhang D, Ye C, Wang Y, Deng X, Deng D, et al. Ultra-sensitive detection of ciprofloxacin hydrochloride in milk by molecularly imprinted electrochemical sensor based on S-CoFe-MOFs/AuNPs. J Food Compost Anal. 2023;122:105439.
14. Shepa J, Király N, Demeterová J, Shepa I, Hviščová P, Volavka D, et al. Determination of ciprofloxacin using metal-organic frameworks-modified electrochemical sensors for environmental and clinical applications. Microchem J. 2025;218:115638.
15. Reddy KR, Brahman PK, Suresh L. Fabrication of high performance disposable screen printed electrochemical sensor for ciprofloxacin sensing in biological samples. Measurement. 2018;127:175-186.
16. Niyitanga T, Evans PE, Ekanayake T, Dowben PA, Jeong HK. Carbon nanotubes-molybdenum disulfide composite for enhanced hydrogen evolution reaction. J Electroanal Chem. 2019;845:39-47.
17. Arrechea S, Guerrero-Gutiérrez EMA, Velásquez L, Cardona J, Posadas R, Callejas K, et al. Effect of additions of multiwall carbon nanotubes (MWCNT, MWCNT-COOH and MWCNT-Thiazol) in mechanical compression properties of a cement-based material. Materialia. 2020;11:100739.
18. Liu H, Jin F, Liu D, Liu W, Zhao J, Chen P, et al. Preparation and electrochemical performance of MWCNT/MoS2 composite modified Co–P hydrogen storage material. Solid State Sciences. 2022;131:106952.
19. Miao Y, Xue F, Zhao J, Li M, Ren K, Wu T, et al. Research and Application of Photoacoustic Transducer Based on MWCNT-MoS_2-PDMS Composite Thin Film Layer. Journal of Physics: Conference Series. 2025;2966(1):012012.
20. Bavandpour R, Rajabi M, Asghari A. Electrochemical determination of epirubicin in the presence of topotecan as essential anti-cancer compounds using paste electrode amplified with Pt/SWCNT nanocomposite and a deep eutectic solvent. Chemosphere. 2022;289:133060.
21. Sohouli E, Ghalkhani M, Zargar T, Ahmadi F. Preparation of a Highly Sensitive Electrochemical Aptasensor for Measuring Epirubicin Based on a Gold Electrode Boosted with Carbon Nano-Onions and MB. Biosensors. 2022;12(12):1139.
22. Wang Y, Xie J, Tao L, Tian H, Wang S, Ding H. Simultaneous electrochemical determination of epirubicin and methotrexate in human blood using a disposable electrode modified with nano-Au/MWNTs-ZnO composites. Sensors Actuators B: Chem. 2014;204:360-367.
23. Hajian R, Mehrayin Z, Mohagheghian M, Zafari M, Hosseini P, Shams N. Fabrication of an electrochemical sensor based on carbon nanotubes modified with gold nanoparticles for determination of valrubicin as a chemotherapy drug: Valrubicin-DNA interaction. Materials Science and Engineering: C. 2015;49:769-775.
24. Nejad FG, Beitollahi H, Sheikhshoaie I. Electrochemical sensing of methotrexate in the presence of folic acid using PAMAM dendrimer-functionalized multiwalled carbon nanotube-modified electrode. Analytical Methods. 2023;15(26):3196-3205.
25. Heydari-Bafrooei E, Askari S. Electrocatalytic activity of MWCNT supported Pd nanoparticles and MoS2 nanoflowers for hydrogen evolution from acidic media. Int J Hydrogen Energy. 2017;42(5):2961-2969.
26. Ibrahim M, Ibrahim H, Almandil NB, Sayed MA, Kawde AN, Aldaqdouq Y. A Novel Platform Based on Au–CeO_2@MWCNT Functionalized Glassy Carbon Microspheres for Voltammetric Sensing of Valrubicin as Bladder Anticancer Drug and its Interaction with DNA. Electroanalysis. 2020;32(10):2146-2155.
27. Dighole RP, Munde AV, Mulik BB, Dhawale SC, Sathe BR. Multiwalled carbon nanotubes decorated with molybdenum sulphide (MoS_2@MWCNTs) for highly selective electrochemical picric acid (PA) determination. Appl Surf Sci. 2024;659:159856.
28. Singh S, Sharma S, Bajwa BS, Kaur I. Hydrothermally synthesized carboxylic acid functionalized multiwalled carbon nanotubes grafted MoS_2 based hybrid composites: Efficient uranium(VI) scavenging sorbents in columns, fabric and matrix membrane systems. Journal of Environmental Chemical Engineering. 2022;10(6):108883.
29. Ramírez-Mondragón E, Contreras OE, Tamayo-Pérez UJ, Oropeza-Guzmán MT. Synthesis and characterization of Ni_2P and MoS_2 on MWCNT as an innovative catalytic material for hydrogen generation. Appl Surf Sci. 2020;503:144163.
30. Khan F, Julien CM, Islam SS. Fabrication of multiwalled carbon nanotubes/MoS_2 nanocomposite: Application as temperature sensor. FlatChem. 2023;40:100521.